PERGAMON

International Journal of Rock Mechanics and Mining Sciences 37 (2000) 705–713

International Journal of
Rock Mechanics
and Mining Sciences

www.elsevier.com/locate/ijrmms

Technical Note

Hugoniot equation of state of the Bukit Timah granite

J.L. Shang[a], L.T. Shen[a], J. Zhao[b,*]

[a]*Laboratory for Non-Linear Mechanics of Continuous Media, Institute of Mechanics, Chinese Academy of Sciences, Beijing, 100080, China*
[b]*Rock Dynamics Group, School of Civil and Structural Engineering, Nanyang Technological University, Singapore, 639798*

Accepted 12 December 1999

1. Introduction

The equation of state (EOS) expresses the relation between the thermodynamic parameters of a material under thermodynamic equilibrium state for the processes which can be continuously realized, such as isothermal and isentropic processes. However, the Hugoniot equation of state represents the locus of all states which can be reached by shocking a material from a given initial state. It is a series of points for which the heat exchange between a system and its surroundings in going from initial to the final state is zero. The Hugoniot EOS is valuable for a wide range of applications, in particular for the consideration of the protection of rock structures from damage induced by an underground explosion, accurate predictions of the effects of the shocks are generally based on a knowledge of the EOS.

Rice et al. [1] discussed strong shock waves in solids and described various experimental techniques by which the dynamic equation of state is measured. With the significant development of measuring techniques and the improvement of measuring accuracy in high velocity impact tests, a great number of test data and the EOS of shock waves have been determined for many materials [2–16].

Kalashnikov et al. [4] made numerous Hugoniot measurements on calcite of various porosities, dolomite and magnesite over the range of 10–120 GPa. Studies on Oakhall limestone, Solenhofen limestone, calcite and other rocks have been conducted at various porosities and saturation conditions [5–11]. Furnish [12] measured the Hugoniot states and release curves for water-saturated and dry Indiana limestone shocked to pressures in the range of 1–10 GPa. Recently, wave profile measurements have been employed by the Sandia National Laboratories [13–15] and the Lawrence Livermore National Laboratory [16].

Usually, gas guns are employed to perform the hypervelocity impact test. Two impact techniques have been developed to measure the dynamic properties of geological materials. One is the reverse target design, which has the sample in the projectile and gives Hugoniot and continuous release information. The other is the forward target design, which has the sample in the target. A window material backs the sample. This formation is useful for measuring loading and Hugoniot information. Furnish [15] has described the characteristics of the two impact techniques in detail.

In this note, the Bukit Timah granite of Singapore is tested under high velocity impact loading. The forward target design has been employed. The note describes the experiment arrangement and test results.

2. Rock material

2.1. Characteristics of rock material

The Bukit Timah granite is of grey colour with patches and spots. Its grain sizes range from 0.2 to 6 mm. The minerals in the sample do not show any orientation. No sign of weathering was detected. Healed fractures or calcite veins are visible. Fig. 1 is a micro-photograph of the granite, and its mineral components are given in Table 1.

Thin section petrographic analyses were conducted. The overall texture of the granite can be characterised

* Corresponding author. Tel.: +65-790-5268; fax: +65-792-1650.
E-mail address: cjzhao@ntu.edu.sg (J. Zhao).

PII: S1365-1609(00)00002-2

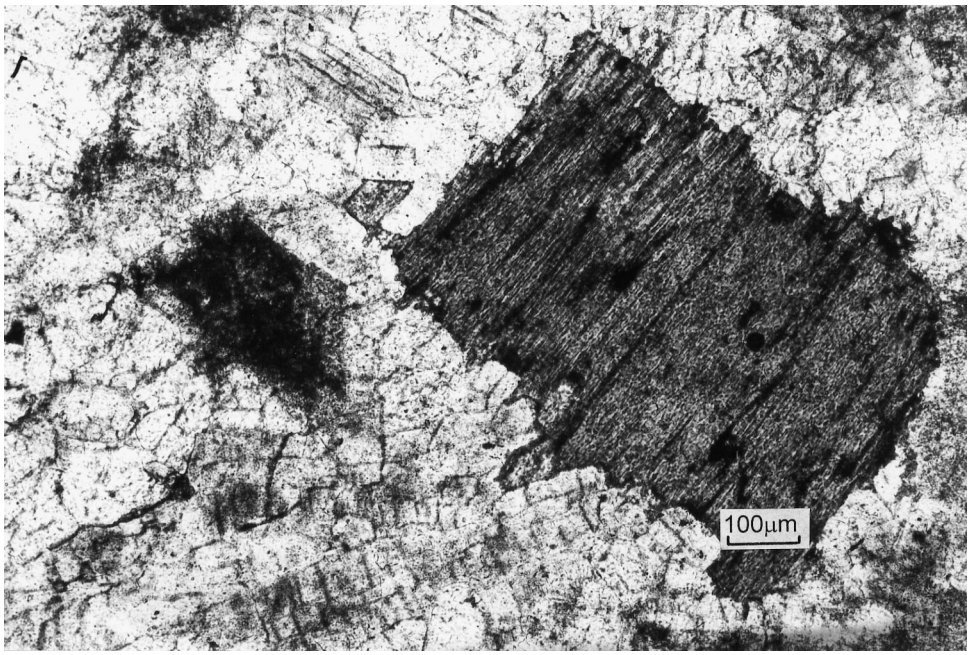

Fig. 1. Microphotograph of the Bukit Timah granite.

by interlocking of a medium-grained groundmass (from 1 × 2 mm to 2 × 3 mm), coarse-grained phenocrysts of quartz (from 1 to 3 mm), and plagioclase feldspars and biotite (from 0.1 × 0.4 mm to 2 × 4 mm). This texture is typical for an intrusive igneous rock. The rock is weakly porphyritic, consisting of phenocrysts up to 3 mm in size enclosed in a medium-grained groundmass.

Observations of the rock sample show micro-fracturing, which seemed to occur during three stages. The earliest micro-fractures are those cutting the phenocrysts of quartz and feldspars, and these are healed and filled mainly by quartz and some feldspars. There is more than one cross-cutting set of such early fractures. These early micro-fractures were observed in the thin sections cut parallel and transverse to the coring direction. The second stage of micro-fracturing is represented by a well defined set of micro-shears, which cut and have displaced phenocrysts of alkali feldspars. The micro-fracturing of the latest stage is randomly distributed in the phenocrysts. They are unhealed and exist more prominently in the thin sections cut along the coring direction.

The mechanical and physical properties of the Bukit Timah granite are shown in Table 2 [17].

Table 1
The mineral components of the Bukit Timah granite

Minerals	Percentages
Quartz	25.4
Alkali Feldspar (sericitised)	20.6
Plagioclase (weakly sericitised)	41.7
Biotite	6.2
Chloritised Biotite	5.0
Sericite	0.5
Opaque	0.3
Epidote	0.3
Zircon, Apatite, and others (not counted)	Trace

2.2. Preparation of specimens

The cylindrical granite cores of 52 mm diameter were obtained through deep drilling. The cores were cut to disks slightly thicker than 2, 4, 6 and 8 mm thickness by a diamond saw. The granite disks were ground and polished to 2, 4, 6 and 8 mm thickness with an error ±0.15 mm. The two surfaces of the granite disks were smooth and the tolerance of the parallelism between the two surfaces is within ±0.05 degrees.

3. Experimental technique

3.1. Rankine–Hugoniot relations

The determination of the state of material behind a

Table 2
Mechanical and physical properties of the Bukit Timah granite

Density	2670 kg/m^3
Sound velocity	5820 m/s
Young's modulus	75.2 GPa
Poisson's ratio	0.16
Uniaxial compressive strength	147.5 MPa
Tensile strength	16.1 MPa

shock front is required to understand the so-called Rankine–Hugoniot relations [18]. Based on the assumption of a one-dimensional, steady-state shock wave, that is, a shock wave whose properties do not vary with time, the Rankine–Hugoniot relations can be written in terms of the variables p, υ, ρ^{-1}, U_s, u_p, and E.

$$\upsilon = \upsilon_0(1 - u_p/U_s) \tag{1}$$

$$p = p_0 + \rho_0 U_s u_p \tag{2}$$

$$E = E_0 + 1/2(p + p_0)(\upsilon_0 - \upsilon) \tag{3}$$

where p is the pressure, ρ is the density, υ is the specific volume, E is the specific internal energy, U_s is the shock wave velocity and u_p is the particle velocity. Subscript 0 refers to the initial state.

There are five variables in the three equations. Only two variables are independent. Therefore, in carrying out shock-wave experiments, it is customary to measure two of the five variables; and from these measurements, the other variables can be calculated.

Extensive single Hugoniot measurements on a large number of substances indicate that for almost all of them, shock velocity (U_s) and particle velocity (u_p) are linearly related. The relation can be expressed as:

$$U_s = C_0 + Su_p \tag{4}$$

where C_0 and S are the material constants.

When p_0, usually equal to one atmosphere, is considered negligibly small compared to p, substituting Eq. (4) into Eqs. (1) and (2), the Hugoniot state equation can be written in following form

$$p = \rho_0 C_0^2 \mu/(1 - S\mu)^2 \tag{5}$$

where

$$\mu = 1 - \upsilon/\upsilon_0 = 1 - \rho_0/\rho \tag{6}$$

Although numerous investigators have expressed their experimental results in the form of Eq. (5), the data can also be expressed, and often are in the purely empirical and analytic form [18]

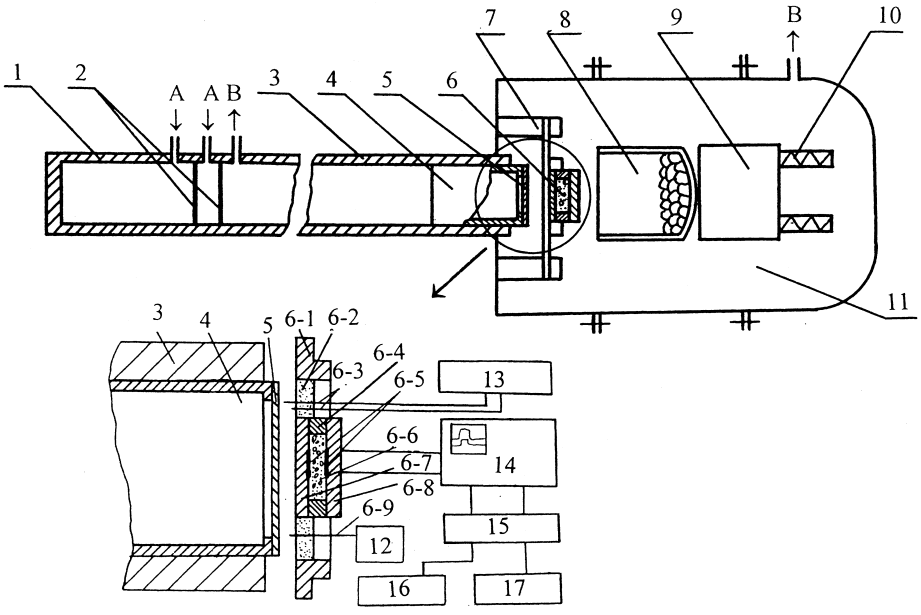

1. Gas chamber
2. Diaphragms
3. Barrel
4. Sabot
5. Flyer
6. Target
6-1. Target ring
6-2. Epoxy
6-3. Velocity pins
B - pumping out
6-4 Protection ring
6-5. Gauge I and II
6-6.Rock specimen
6-7. Cover plate
6-8. Back plate
6-9. Trigger pin
7. Target holder
8. Catcher tube
9. Heavy block
10. Hydraulic spring
11.Expansion chamber
12. Power supply
13. Timer
14.Digital oscilloscope
15. Computer
16. Printer
17. Ploter
A - gas in

Fig. 2. Schematic of light gas gun, assembly of target and instrumentation system.

$$p = A\mu + B\mu^2 + C\mu^3 \quad (7)$$

where A, B, and C are material dependent constants.

3.2. Impact apparatus

The impact tests were conducted using a light gas gun of 101 mm internal bore diameter [19]. A schematic of the light gas gun is shown in Fig. 2. This gun has a double diaphragm breech and uses compressed nitrogen (impact velocity <600 m/s) or compressed hydrogen (impact velocity >600 m/s) as driving gas. The type and pressure of the compressed gas are chosen according to the desired impact velocity. Once a working pressure of the driving gas is identified, suitable diaphragms can be determined accordingly. The diaphragms are selected to withstand slightly more than half the working pressure in gas chamber and to open cleanly and quickly when subjected to full pressure. Annealed aluminium diaphragms and stainless steel diaphragms are used in these experiments. Firing is accomplished by exhausting the region between the diaphragms (initially pressurized to half working pressure) so that each diaphragm in turn experiences the

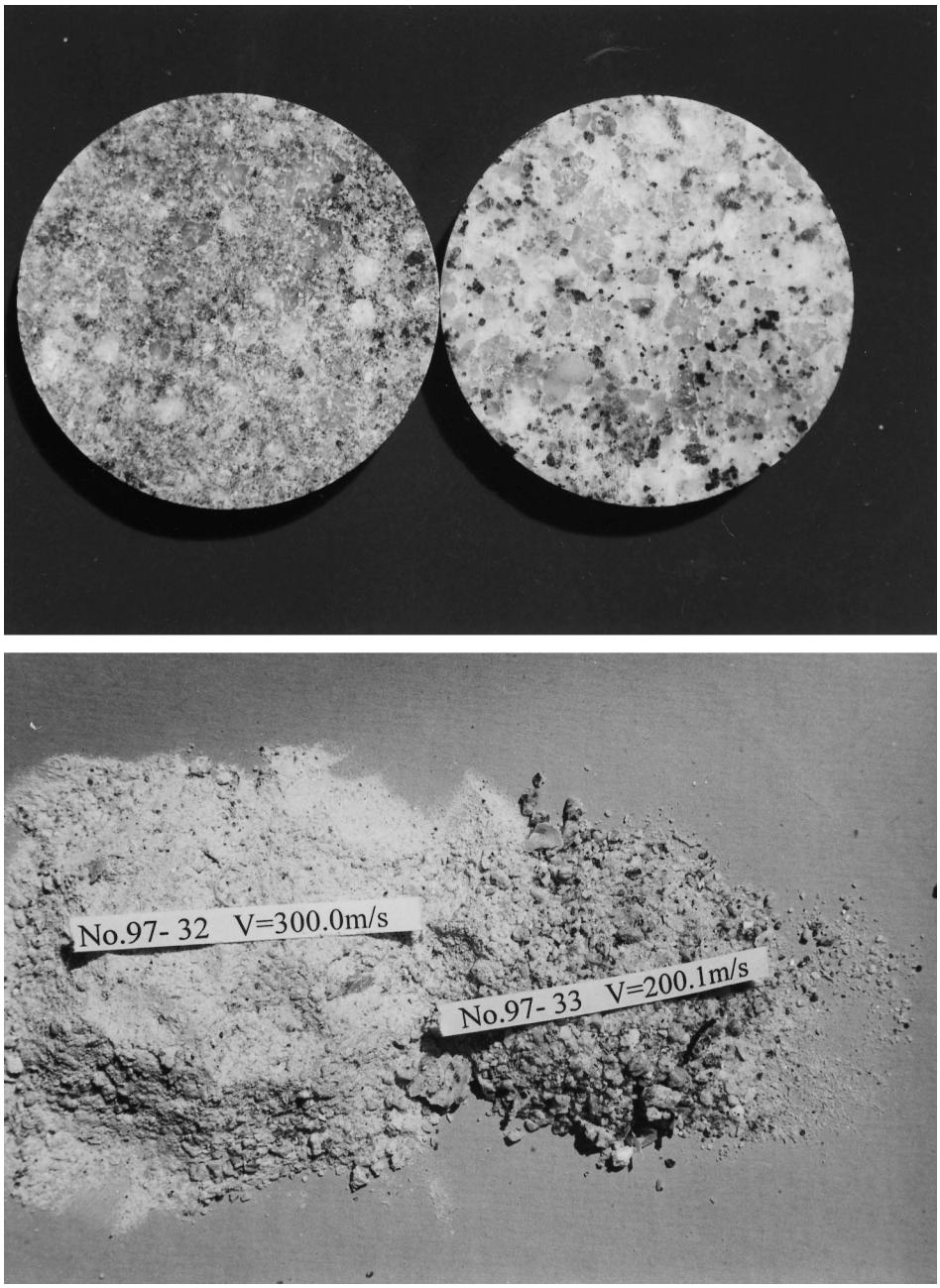

Fig. 3. Granite specimens before and after impact tests.

full pressure and is broken. The pressured gas is released and pushes the projectile to accelerate along the barrel. Eventually, the projectile impacts the target at the muzzle.

Before impacting, the target assembly is placed into the target holder and the whole light gas gun system is sealed and vacuumed. The vacuumed pressure in the system is maintained at less than 1 Pa before shooting. Meanwhile, in order to prevent the projectile from moving, the space between the rear part of projectile and the diaphragm is firstly vacuumed. The objectives of vacuuming are:

1. to reduce the air resistance to the motion of the projectile;
2. to avoid the frictional heat that may melt the "O" ring around the projectile and hence pollute the barrel;
3. to avoid an air cushion forming by accumulation of air in the front of the accelerated projectile.

In order to ensure planar impact, the target holder is composed of three differential screw apparatuses that can be adjusted to maintain the tilt angle between the target plane and the impact plane of the projectile at

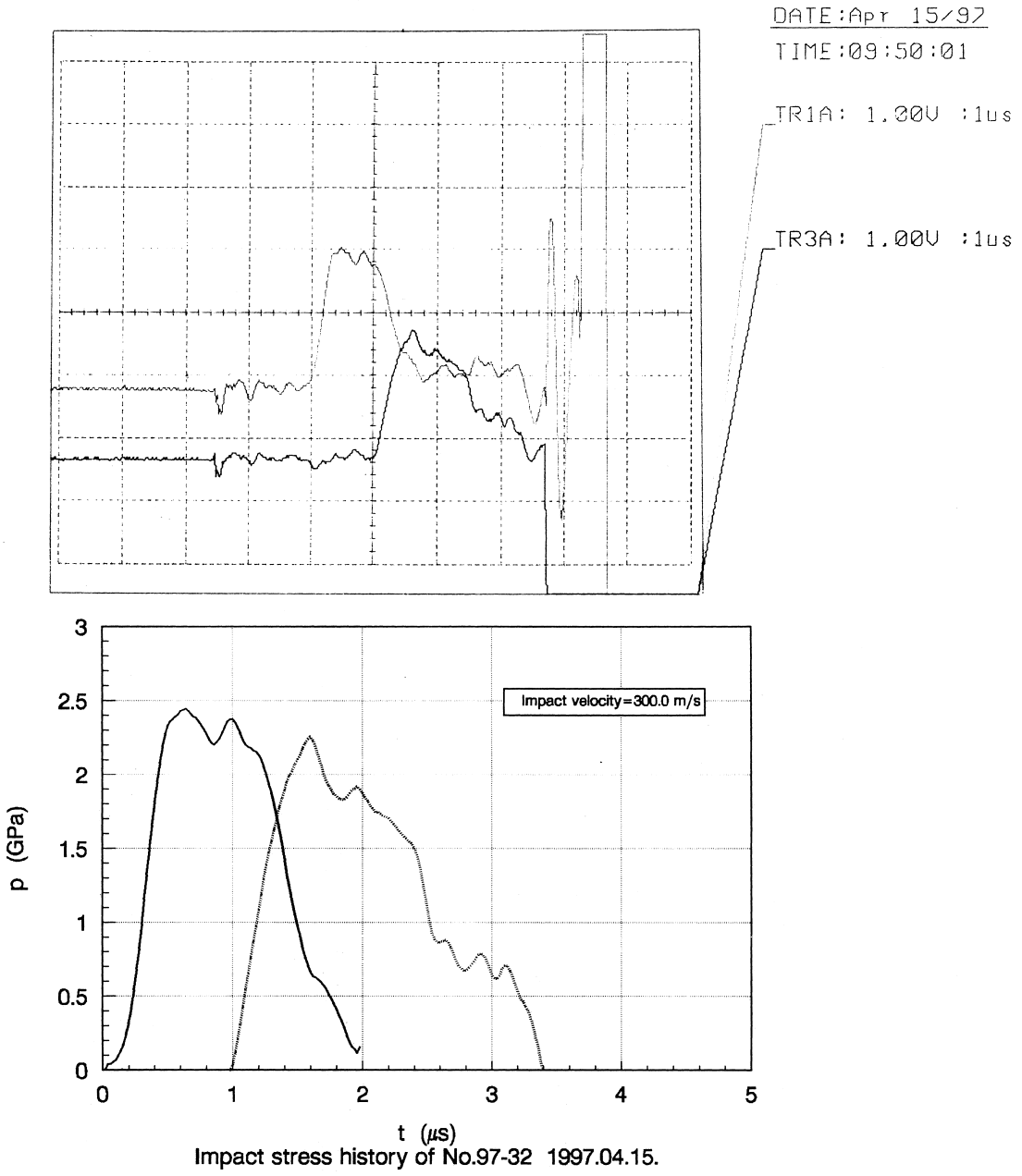

Fig. 4. Typical profiles of stress waves recorded during impact tests.

less than 10^{-3} rad. The assembly of target and the instrumentation system used to measure and record the wave profiles and data are also shown in Fig. 2.

Fig. 3 shows the granite specimens before and after the impact tests.

3.3. Forward target design

The forward target design is employed in this impact test, as shown in Fig. 2. Aluminium alloy (2024 Al) is used as the flyer, the front cover, the back cover and the protection ring. The nominal thickness of the flyer is 4 ± 0.1 mm. The use of 2024 Al is based on two considerations: its Hugoniot parameters are known [2], ($U_s = 5328 + 1.338\ u_p$, $\rho = 2.7$ g/cm^3); and its impedance is close to that of the granite. Two axial electrical pins are installed to measure the velocity of impact. Two stress gauges are attached on the front and back of the rock specimen. The insulation between the stress gauge and the 2024 Al plates is achieved by adding a 25 μm thickness Mylar membrane.

When the stress wave induced by the impact travels in the rock specimen along the axial direction from the front to back, the two gauges record the interval time of the shock wave traveling through the thickness of the rock specimen and the history of the impact stress on the respective sides. One set of the parameters of the Hugoniot state equation of the granite — obtained by means of two groups of data (U_s , u_p) and (P, u_p) and checkable with each other — can be determined in one shoot based on the recorded impact velocity (V_0), the average shock speed (U_s), the amplitude of the impact stress (p) and the Hugoniot parameters of the 2024 Al. A group of such data can be obtained by a series of the impact tests with various impact velocities. Correspondingly, the Hugoniot state equation of the granite can be derived through a regression method.

The function of the 2024 Al protection ring is to ensure that the lateral release waves from the periphery do not interfere with the measurement at the centre, and guarantee that the data acquisition by the stress gauges is under a uniaxial strain condition. Although the aspect ratios (diameter/thickness) of the sample assembly (4:1 to 5.8:1) are sufficiently large [16], the wave profile cannot be easily obtained without the protection ring. The unevenness of the surfaces of the components such as that of flyer, the cover plate, the back plate and the granite specimen are limited within 2 μm. A silicon grease is smeared on the contact surfaces of the cover plate, the back plate and the specimen. A small load is applied when the specimen is assembled. All of these measures are to ensure good contact between the specimen and the plates.

The stress gauges used in this experiment were manufactured by the Red Star Strain Gauge Factory of China, (type MBP50-6BD-45). The sensitive element is a 6 mm diameter spiral grid and the nominal resistance

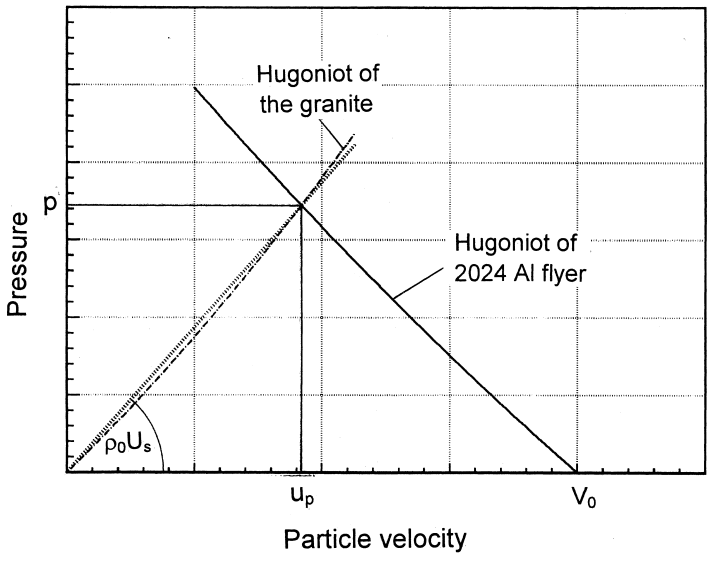

p — Pressure at the interface between 2024 Al plate and granite specimen
u_p — Particle velocity of the granite specimen,
U_s — Shock velocity in the granite specimen,
ρ_0 — Initial density of the granite,
V_0 — Impact velocity.

Fig. 5. Impedance match solution of the Hugoniot measurement.

Table 3
Summary of the test data

Test no.	Impact velocity V_0 (m/s)	Impact stress p (MPa)	Thickness of specimen δ (mm)	Interval time shock from gage1 to 2, ΔT (μ_s)	Velocity of shock wave U_s (m/s)			Particle velocity u_p (m/s)			Bulk strain $\mu=1-\rho_0/\rho=u_p/U_s$ ($\times10^{-4}$)
					Calculated based on V_0 and p	$\delta\Delta T$	Relative error (%)	Calculated based on V_0 and p	Calculated based on V_0, δ, ΔT	Relative error (%)	
97-23	65.1	496	7.94	1.32	6011	6015	−0.07	30.9	30.7	0.65	51.41
97-22	71.6	544	6.04	1.00	5975	6040	−1.10	34.1	33.7	1.17	57.07
97-26	71.8	548	5.78	0.96	6019	6020	−0.02	34.1	33.9	0.59	56.65
97-31	91.2	694	7.88	1.30	5971	6061	−1.50	43.5	42.9	1.38	72.90
97-36	92.1	695	5.82	0.96	5863	6063	−3.40	44.4	43.4	2.25	75.73
97-30	101.6	785	8.02	1.30	6151	6169	−0.29	47.8	47.3	1.05	77.71
97-25	102.6	796	8.00	1.30	6211	6154	0.92	48.0	48.0	0.00	77.28
97-24	118.3	916	7.98	–	6170	–	–	55.6	–	–	90.11
97-29	207.2	1676	6.04	0.92	6684	6565	1.78	93.9	94.3	−0.43	140.51
97-32	300.0	2422	6.06	0.96	6564	6313	3.82	138.2	140.2	−1.45	210.54
97-34	308.2	2426	8.00	1.28	6215	6259	−0.56	146.2	144.9	0.89	235.24
97-42	422.6	3357	4.02	–	6240	–	–	201.5	–	–	322.92
97-44	495.7	4092	4.00	0.60	6690	6667	0.34	229.1	228.2	0.39	342.45
97-38	505.5	4192	6.08	0.92	6744	6609	2.00	232.8	233.9	−0.47	345.20
97-48	627.2	5261	4.06	0.60	6795	6767	0.41	290.0	289.0	0.34	426.78
97-41	685.0	5791	5.96	–	6853	–	–	316.5	–	–	461.84
97-46	793.9	6760	5.98	–	6856	–	–	369.3	–	–	538.65
97-47	801.3	6990	6.04	–	7202	–	–	363.5	–	–	504.72

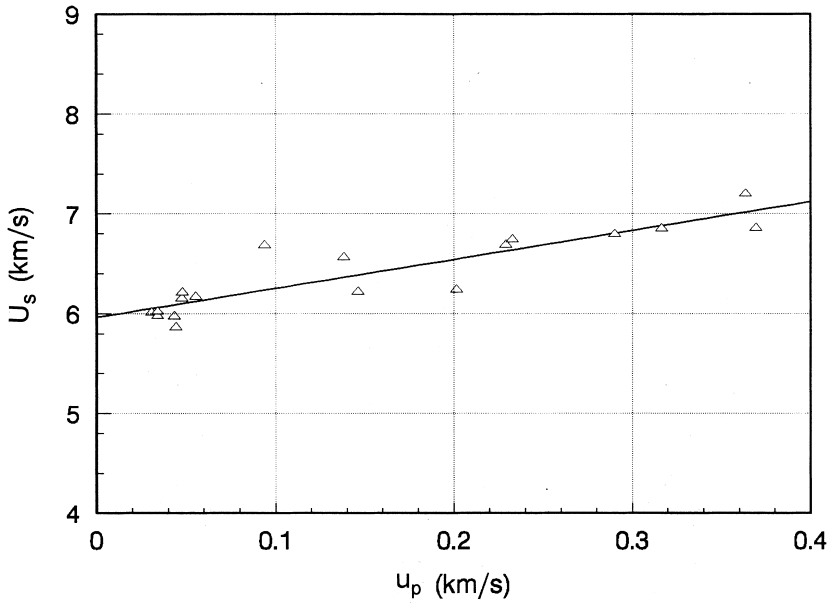

Fig. 6. Linear Hugoniot relation for the Bukit Timah granite.

is 50 $\Omega \pm 1\%$. A pulse power unit was used to supply the gauge with the pulse voltage. All the details of principle and structure of the pulse power can be found in [20]. The start of the power source is controlled by a silicon controlled rectifier which is connected to the trigger pin. The measuring range of the MBP50-6BD-45 gauge is between 50 MPa and 20 GPa and the piezoresistivity coefficient k of the gauge has values as follows:

$k = 0.0260\ \text{GPa}^{-1}$ (< 3 GPa)

$k = 0.0285\ \text{GPa}^{-1}$ (> 3 GPa)

Fig. 4 shows typical profiles of the stress waves recorded by the stress gauge.

4. Results

Eighteen acceptable experiments were conducted in this study and the relevant experimental results are given in Table 3. The range of impact velocity in the tests is from 65 to 800 m/s, and the corresponding impact stress range is from 500 MPa to 7 GPa. Based on the experimental data of impact velocities, impact stresses and the Hugoniot parameters of 2024 Al, a

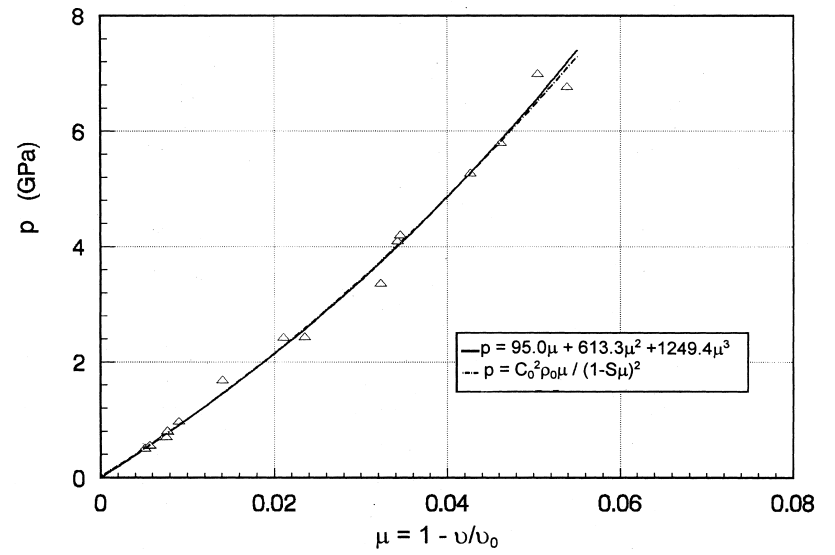

Fig. 7. Impact stress–bulk strain curve for the Bukit Timah granite.

series of shock velocities U_s and particle velocities u_p of the granite can be calculated by the impedance matching method (see Fig. 5). The Hugoniot linear relation of the Bukit Timah granite is fitted as follows

$$U_s = 5961 + 2.907u_p \quad (8)$$

The coefficient of regression $r = 0.8935$. Fig. 6 shows the Hugoniot linear relation of the granite material.

Another group of the shock velocities (U_s) and particle velocities (u_p) of the granite is also given in Table 3. In this group of (U_s, u_p), U_s is obtained from $\delta/\Delta T$ (δ is the thickness of the rock specimen, ΔT is the interval time for shock wave traveling through the thickness δ); u_p is calculated based on the impact velocity V_I, shock velocity (U_s) and the continuity conditions of the pressure and velocity at the interface. The maximum deviation of (U_s) and (u_p) between the two groups of (U_s, u_p) is 3.82% and 2.34% respectively.

Bulk strains obtained directly from the tests are listed in Table 3. For convenience of engineering application, the relation between the pressure p and the bulk strain μ regressed from the test data is into the form of Eq. (7)

$$p = 95.0\mu + 613.3\mu^2 + 1249.4\mu^3 \quad (9)$$

The curve of $p-\mu$ for the granite is shown in Fig. 7. In the figure, the dashed line is plotted based on the regression Eq. (9) and the solid line is from Eq. (5). The two lines are in good agreement. This means that the regression accuracy of the quadratic polynomial is sufficient good. However, some scattered test results can be seen in Figs. 5 and 6. They arise from the following aspects:

1. the error in measuring stress amplitude due to the existence of $\pm 6\%$ discord between the stress gauges;
2. $\pm 1\%$ measurement error of impact velocity; and
3. heterogeneity, anisotropy and the coarse grain size of the granite.

5. Conclusions

The Hugoniot equation of state of the Bukit Timah granite was determined through impact experiments using a light gas gun. The range of impact velocity was from 65 to 800 m/s and the corresponding impact stress range from 0.5 to 7 GPa. The forward target design was employed. The linear Hugoniot relation between the shock velocity (U_s) and the particle velocity (u_p) of the granite follows the form:

$$U_s = 5961 + 2.907\ u_p \text{ (m/s)}$$

The quadratic polynomial representing the relation between the impact stress (p) and the bulk strain ($\mu = 1-\upsilon/\upsilon_0$) regressed from the test results is in the form:

$$p = 95.0\mu + 613.3\mu^2 + 1249\mu^3 \text{ (GPa)}$$

References

[1] Rice MH, McQueen RG, Walsh JM. Compression of solids by strong shock waves. New York: Academic Press, 1958.
[2] McQueen RG, Marsh SP, Taylor JW, Fritz JN, Carter WJ. The equation of state of solid from shock wave studies. In: Kinslow R, editor. High Velocity Impact Phenomena. New York: Academic Press, 1970. p. 293–417.
[3] Johnson JD, Bennett B. In: Handbook of Material Properties Data Bases, Vol.1c Equation of State. Los Alamos National Laboratory, 1985.
[4] Kalashnikov NG, Pavlovskiy MN, Simakov GV, Trunin RF. Dynamic compressibility of calcite-group minerals. Phys Solid Earth 1973;2:80–4.
[5] Murri WJ, Grady DE, Mahrer KD Internal Report, SRI, 1975.
[6] Grady DE. Shock deformation of brittle solids. Int J Impact Engng 1980;14:913–24.
[7] Grady DE Technical Report SAND83-0370, Sandia National Laboratory, 1983.
[8] Grady DE, Murri WJ, DeCarli P. Hugoniot sound velocities and phase transformations in two silicates. J Geophys Res 1975;80:4857–61.
[9] Grady DE, Moody RL, Drumheller DS Technical Report SAND86-2110, Sandia National Laboratory, 1986.
[10] Schuler KW, Grady DE. Compression wave studies on Solenhofen limestone. In: Technical Report SAND76-0279, Sandia National Laboratory, 1979.
[11] Swegle JW. Irreversible phase transitions and wave propagation in Silicate geologic material. J Appl Phys 1990;68:2220–32.
[12] Furnish MD. Dynamic compression and release experiments of Indiana limestone. In: Schmidt SC, Johnson JN, Davison LW, editors. Shock Compression of Condensed Matter. Amsterdam: Elsevier, 1989. p. 625–8.
[13] Furnish M Technical Report SAND90-1317, Sandia National Laboratory, 1990.
[14] Furnish M Technical Report SAND92-0984, Sandia National Laboratory, 1992.
[15] Furnish M. Recent advances in methods for measuring the dynamic response of geological materials to 100 GPa. Int J Impact Engng 1993;14:267–77.
[16] Erskine D, Nellis WJ, Weir ST. Shock wave profile study of tuff from the Nevada test site. J Geophys Res 1994;99:15529–37.
[17] Zhao J, Zhou Y, Sun J, Low BK, Choa V. Engineering geology of the Bukit Timah granite for underground cavern construction. Q J Engng Geol 1995;28:153–62.
[18] Rinehart JS. In: Stress Transients in Solids. New Mexico: Santa Fe, 1975. p. 113–31.
[19] Zhao SD, Shen LT, Zhao SL. A single-stage light gas gun for impact studies. Acta Armamentarii 1985;4:49–54.
[20] Oved Y, Luttwak E, Rosenberg Z. Shock wave propagation in the Layered composites. J Composite Materials 1978;12:84–96.